

Distribution of Grain Boundary Planes and Misorientations in Magnesium Oxide

D.M. Saylor¹, A. Morawiec², G.S. Rohrer¹, S. Mahadevan³, and D. Casasent³

¹Materials Science and Engineering Dept., Carnegie Mellon University, Pittsburgh, PA 15213, USA

²Instytut Metalurgii i Inżynierii, Materialowej PAN, Reymonta 25, 30-059 Krakow, Poland

³Electrical and Computer Engineering Dept., Carnegie Mellon University, Pittsburgh, PA 15213, USA

Keywords: grain boundaries, misorientation, microstructure, grain boundary distribution, magnesium oxide.

Abstract. We have developed a technique that allows the geometry and crystallography of large quantities of contiguous crystallites to be accurately characterized. Using this technique, in concert with high precision serial sectioning, we have extracted the geometric and crystallographic configuration of approximately 2.5 mm² of grain boundary area in a 0.33 mm³ volume of polycrystalline magnesium oxide. Using these data, we have specified the distribution of grain boundaries within the five-dimensional space of misorientation and inclination types. The data show that in addition to the texture in the misorientation space induced by processing, there is texture in the space of grain boundary planes. For example, for 5 ° misorientations about <111>, pure twist and tilt boundaries occur more frequently than general boundary plane configurations.

1 Introduction

There are five mesoscopically observable characteristics of a grain boundary: three that describe the lattice misorientation and two that describe the boundary inclination. While the distribution of lattice misorientations is frequently derived from the analysis of planar sections, grain boundary inclinations are rarely reported for more than a handful of boundaries [1-3]. In a recent paper, we

characterized the five mesoscopically observable parameters for 4665 grain boundaries in a magnesia polycrystal. However, the grain boundaries in this data set were restricted to those meeting at triple junctions, and did not represent the true distribution of grain boundaries. The purpose of the present paper is to describe an automated technique that allows the geometry and crystallography of large quantities of contiguous crystallites to be accurately characterized. Using this technique, along with high precision serial sectioning, we have extracted the crystallographic and geometric configuration of the three-dimensional grain boundary network in a magnesia polycrystal and specified the distribution of grain boundaries in the space of the five mesoscopically observable parameters.

2 Experimental Procedure

Acquisition of the geometric and crystallographic data required to accurately characterize the mesoscopic grain boundary parameters requires orientation measurements with high spatial resolution from multiple sections through the sample. This was accomplished using an automated scanning electron microscope (SEM) mapping system that controls both the stage and beam position as well as the acquisition of images and electron backscattered diffraction patterns (EBSPs). When the mapping is conducted, the sample surface is initially divided into sectors. At each sector, a secondary electron image is recorded, and EBSD measurements of crystallite orientation are made at regular intervals within the sector. When the sector characterization is complete, the microscope stage is automatically moved to the next sector. The entire procedure is carried out under computer control. Because we use SEM images to determine grain boundary positions, the orientation measurements can be conducted at relatively coarse intervals. Thus, compared to the conventional OIM methods, we are able to resolve the boundary positions accurately without accumulating redundant orientation data [6]. After an area is mapped, high precision serial sectioning is used to remove a thin layer and the process is repeated so that the three-dimensional characteristics of the grain boundary network can be determined.

The experiment described here was carried out on polycrystalline magnesia with a 109 μm grain size that was described in detail elsewhere [4]. For the present paper, it is useful to note that hot pressing during the processing of this material induced a $\langle 111 \rangle$ axial texture that was 11 times random at the maximum. The sample was coated and tilted at 60° in the SEM for imaging and acquisition of the EBSPs. On each layer, a scan area consisting of a 14 x 14 grid of sectors was characterized. In each of the 196 sectors, a tilt-corrected image was taken at 750x

magnification, and 300 uniformly distributed orientation measurements were recorded. After the scan, approximately $7\mu\text{m}$ of material was removed and the entire process was repeated until data from five layers was accumulated.

2.1 Reconstruction of the grain boundary network

The initial step in reconstructing the grain boundary network from the recorded data is to combine the SEM images and crystallite orientation measurements to produce high-resolution orientation maps. After correcting spatial distortions in each SEM image, the relative positions of the images in each layer were determined using the algorithm described by Mahadevan and Casasent [7]. Next, the grain boundaries in each sector image were digitized by hand. The relative positions of images were then used to construct large mosaic maps of the grain boundaries and orientation measurements on each layer. To produce orientation maps from these data, every grain in the scan area, defined by contiguous pixels not associated with a grain boundary, was identified and assigned an orientation. Because multiple orientation measurements were made in each grain, minority orientations resulting from errors in the indexing had to be excluded. The remaining majority orientations, which contained some scatter, were averaged to make the final orientation assignment for each grain [8].

Once the high-resolution orientation maps from each layer were obtained, it was necessary to align the maps to establish the same reference frame for all layers. Here, we chose the first layer as the global reference frame. The transformation from all subsequent layers to the first layer is given by $\mathbf{A}\mathbf{x}+\mathbf{t}$ where \mathbf{x} is a two dimensional vector which represents the position within a given layer, \mathbf{A} is a 2×2 affine transformation matrix, and \mathbf{t} is a two dimensional translation vector. To find (\mathbf{A},\mathbf{t}) for each layer, we initially find (\mathbf{A},\mathbf{t}) that maximizes the area of overlap between positions with the same orientations on adjacent layers. We then use the (\mathbf{A},\mathbf{t}) describing the transformation that aligns adjacent layers to calculate the (\mathbf{A},\mathbf{t}) that aligns each layer with the initial layer.

After all layers were transformed into the global reference frame, the common grains through all the layers were identified using the following algorithm. The area of overlap between all grain pairs on adjacent layers was determined. The pair of grains that has the largest area of overlap is identified as being two sections of the same grain. The pair with the second largest area of overlap is then assigned in the same way. The process continues until all grains have been assigned or do not overlap any grains that have not been assigned. The success of this algorithm, which we have found to be 99.5% accurate, derives from the fact that the distance between adjacent layers is much smaller than the average grain

size. After the grains were identified on all layers, pixels associated with common grain boundaries on adjacent layers were used to create a meshed interfacial surface of triangular elements. The orientations of the crystallites were then reassigned by repeating the process that was used in each layer, but considering all of the orientation data from different section planes of the same grain.

2.2 Grain boundary distribution

After all boundaries were meshed, it was possible to determine the distribution of grain boundaries over all five mesoscopically observable parameters. Using the vertices of the triangles in the mesh, the area and normal vector for each triangle were determined. Next, the normal vector and the orientations of the crystallites bounding each triangle were used to specify all five grain boundary parameters, and the total boundary area associated with each discrete grain boundary can be calculated. The space of grain boundaries is discretized in the following manner. The misorientations, each described by three Eulerian angles (ϕ_1, Φ, ϕ_2) , were parameterized by ϕ_1 , $\cos(\Phi)$, and ϕ_2 in the range of zero to $\pi/2$, 1, and $\pi/2$, respectively. The inclinations, described by two spherical angles, θ and ϕ , were parameterized by $\cos(\theta)$ and ϕ in the range of zero to 1 and 2π , respectively. This domain of grain boundary space was tessellated into cells by dividing the range of each parameter into twelve equal partitions, a resolution of approximately 7.5° , each cell representing a discrete grain boundary type. Within this domain, 36 symmetrically equivalent grain boundaries exist for each characterized grain boundary. Thus, the area of each triangle in the mesh is associated with 36 cells within the domain.

3. Results and Discussion

We have characterized all five macroscopic degrees of freedom for approximately 2.5 mm^2 of grain boundary area in a 0.33 mm^3 volume. For every misorientation and inclination pair, there are 36 equivalent pairs in our domain of grain boundary types. Thus, after specifying a misorientation, the value of the distribution at every inclination is taken as the average of all 36 symmetrically equivalent misorientation and inclination pairs. These averaged values for the inclination parameters are then plotted on an inverse pole figure.

The distribution of misorientations alone, averaged over the space of inclinations, exhibited a strong peak at low angle misorientations (\approx random at maximum). Furthermore, large angle misorientations ($>15^\circ$) were primarily restricted to those

described by rotations about $\langle 111 \rangle$ due to the sample's axial texture. Fig. 1 shows the distribution of inclination parameters for two fixed misorientations. These plots show strong texture over the inclination parameters. In (a), there appears to be a preference for either pure twist or pure tilt inclinations. There is a strong peak in the distribution at $\langle 111 \rangle$, the pure twist boundary. Furthermore, there appears to be a wide band of relatively high concentrations 90° from $\langle 111 \rangle$, or the pure tilt boundaries, with broad peaks centered on tilt boundaries with $[110]$ planes. In (b), we see that there is a broad minimum at $\langle 111 \rangle$ and maxima in the vicinity of tilt boundaries with $[211]$ planes.

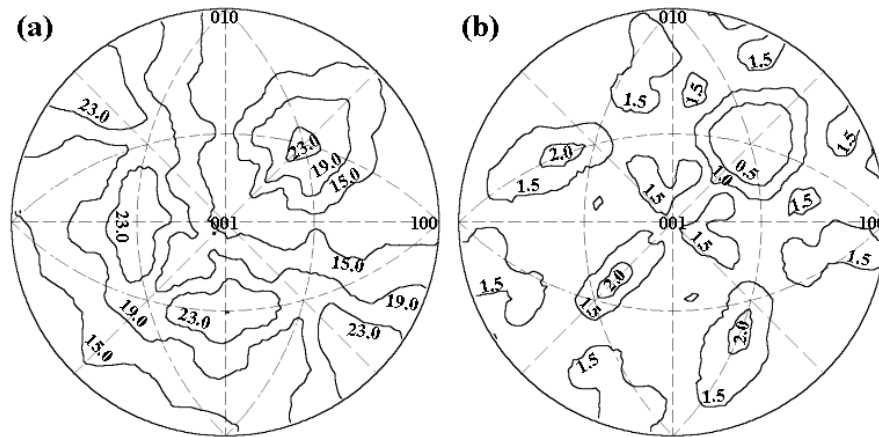


Fig. 1. Distribution of grain boundary inclinations for lattice misorientations corresponding to rotations of (a) 5° about $\langle 111 \rangle$ and (b) 60° about $\langle 111 \rangle$ ($\Sigma 3$). Contour values are in multiples of a random distribution.

The plots in Fig. 1 represent a small fraction of the entire grain boundary space. However, the apparent trend of preferred inclinations is typical of any of the distributions we have examined at fixed misorientation. While it is well known that grain boundary misorientations are not necessarily distributed randomly over the domain of possibilities, the current results illustrate that the inclinations of the grain boundaries can also exhibit texture. This observation provokes a number of interesting questions regarding the origin of this texture, its relation to the properties of the boundaries, and how it might be controlled. For example, are certain points in the inclination space preferentially occupied because they represent low energy configurations or because these boundaries move more slowly and are eliminated with a lower probability? We intend to address this and other questions in a forthcoming paper that will provide a more complete

description of the distribution of grain boundaries over the five mesoscopically observable parameters.

4. Summary

We have developed an experimental technique that allows the geometry and crystallography of large quantities of contiguous crystallites to be characterized. Data extracted from the analysis of 2.5 mm^2 of grain boundary area in a volume of 0.33 mm^3 has enabled us to specify the distribution of grain boundaries over all mesoscopic parameters. We find that strong texture exists in the space of grain boundary inclinations, a domain that has not been previously explored.

Acknowledgement

This work was supported primarily by the MRSEC program of the National Science Foundation under Award Number DMR-0079996.

References

- [1]
- [2]
- [3]
- [4] D.M. Saylor, A. Morawiec, B.L. Adams, and G.S. Rohrer, *Interface Science*, **8**, 131-40 (2000).
- [5]
- [6] B.L. Adams, S.I. Wright, and K. Kunze, *Met. Trans.*, **24A**, 819-831 (1993).
- [7] S. Mahadevan ..
- [8] A. Morawiec